ACS Sustainable Resource Management

pubs.acs.org/acssrm

Article

Upcycling of Waste Polymer Using Surface Modified Hemp Derived Biochar Carbon for Sustainable Packaging Applications

Gautam Chandrasekhar, Kearston Edwards, Desmond Mortley, and Vijaya Rangari*

Cite This: *ACS Sustainable Resour. Manage.* 2024, 1, 625−633

Read Online

ACCESS | Metrics & More | Article Recommendations

Downloaded via UNIV OF ALABAMA HUNTSVILLE on December 18, 2024 at 19:08:07 (UTC).
See https://pubs.acs.org/sharingguidelines for options on how to legitimately share published articles.

ABSTRACT: Out of 300 million tons of plastics produced globally, only 10% are being recycled. Due to this, there is always a demand for alternative, effective methods to cope with this low recycling rate of plastics. This work demonstrates such an effective technique for recycling high-density polyethylene (HDPE) wastes, incorporating biochar synthesized from postharvest hemp crop residue as fillers. Generally, carbon-based materials are considered to have inert surface properties. However, hemp-derived carbon was successfully functionalized in this work using low-temperature plasma (LTP) treatment in the presence of sulfur hexafluoride (SF_6) gas. Changes such as the presence of fluorine functional groups and alterations in the surface morphology, which resulted in surface area enhancement, were observed with the LTP treatment. An X-ray diffraction study of the carbon samples revealed the formation of a new peak at 18.98°, which corresponds to the [002] lattice planes because of the LTP treatment. The presence of fluorine in the LTP-treated carbon samples was confirmed with X-ray photoelectron spectroscopy and Fourier transform infrared spectroscopy. The composite films reinforced with LTP-treated carbon had a significant increase in crystallinity percentage and mechanical properties compared to those of films reinforced with untreated carbon. The HDPE/carbon films loaded with 1 wt % of LTP-treated carbon had superior mechanical and thermal properties compared to the rest of the samples. Compared to HDPE films without any carbon fillers, the HDPE/carbon films loaded with 1 wt % LTP-treated carbon significantly improved elastic modulus and maximum tensile strength by around 3.4 times and 3.7 times, respectively. However, when compared to the neat HDPE film, there was a significant drop in the ability to strain with the LTP-treated, carbon-loaded film samples. The overall crystallinity of HDPE increased by a maximum of 43.8% by the addition of LTP-treated carbon. The LTP treatment was found to be effective in enhancing the interfacial adhesion of carbon and its interaction with the HDPE matrix.

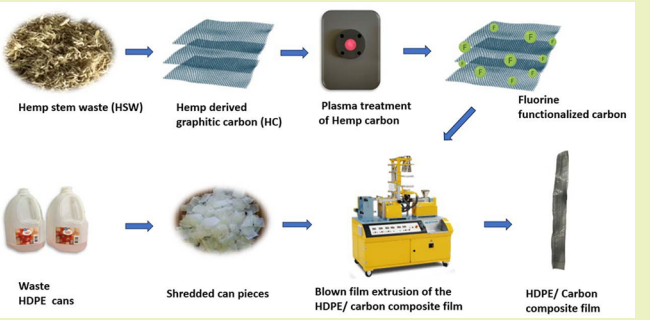

KEYWORDS: *low-temperature plasma treatment, high-density polyethylene, hemp-derived carbon, plastics recycling, carbon interfacial adhesion*

INTRODUCTION

Plastic materials have played a significant role in the global development. It has helped humans in their daily lives to meet various needs ranging from very basic to advanced applications.[1] Over time, the usage and production of plastics have grown exponentially and reached a point where the waste associated with plastics is no longer disposed of properly.[2,3] As reported by the United States Environmental Protection Agency in 2017, the recycling rate of plastic waste from the total plastic produced in the U.S. is 8.8%.[4] The major share of the waste is from the packaging sector with polymers such as polyethylene (PE), high-density polyethylene (HDPE), poly(ethylene terephthalate) (PET), and polypropylene (PP). The recycling rate of HDPE natural bottles in 2018 was only 29.3%. Due to these serious concerns associated with plastic waste disposal, researchers are actively working on enhancing the circular economy and sustainability of waste plastics. Common types of recycling techniques are primary recycling, secondary recycling, tertiary recycling, quaternary recycling, and chemical recycling.[5] Improving properties of waste plastics by the reinforcement of fillers such as wood dust and biochar have also gained a lot of attention in plastic waste upcycling.[6]

HDPE is a common thermoplastic composed of large molecules of carbon and hydrogen atoms. HDPE is commonly synthesized by converting methane arising from fossil fuels by applying heat and pressure. Approximately 1.75 kg of petroleum is considered necessary to make 1 kg of HDPE.

Received: September 7, 2023
Revised: March 21, 2024
Accepted: March 27, 2024
Published: April 9, 2024

ACS Publications

© 2024 American Chemical Society

https://doi.org/10.1021/acssusresmgt.3c00041
ACS Sustainable Resour. Manage. 2024, 1, 625−633

So, depending on virgin HDPE instead of repurposing waste HDPE is not at all a sustainable option. HDPE, being a polymer that has relatively low branching, helps itself to build strong intermolecular forces and tensile strength. Due to its excellent mechanical, thermal, and chemical properties, it is widely used to make packaging materials such as water cans, milk bottles, storage bins, bags, etc. HDPE is considered the third most used commodity among the thermoplastic polymers in use globally after PVC and PP, so considering the humungous HDPE wastes generated globally, there is a relevant necessity for deriving alternate effective ways for managing these wastes.[7,8]

Similar to plastic waste, agricultural waste is also a global concern. Agricultural production must cope with the exponentially increasing demand for food to satisfy the fast-growing population. However, abundant amounts of agricultural waste are also being generated and lack proper management. When agricultural crop waste disposal becomes a crisis, farmers are forced to burn them, which creates serious global air pollution. In India, the estimation is that 18−30% of crop residue is disposed of by burning, which causes emissions of various pollutants, including greenhouse gases. Even though countries have started banning these practices, most of them are still prevailing.[9,10] Among various techniques used for crop residue management, pyrolysis is considered a viable option due to its low carbon footprint and environmental harm.[11] In pyrolysis, agricultural wastes are subjected to elevated temperatures in an oxygen-free environment. The major products generated after the pyrolysis of lignocellulosic agricultural wastes are biochar and bio-oil.[12] In recent years, as the reduction of greenhouse emissions became a priority, the synthesis of biochar from lignocellulosic biomass has gained much attention among researchers. Biochar is a carbon-rich material with superior properties such as high surface area, porosity, high thermal stability, and electrical conductivity. It is used for diverse applications such as water filtration,[13] reinforcement fillers,[14] and energy storage devices.[15]

Among popular agricultural crops, hemp crop is a quick-growing crop that needs relatively low maintenance and caters to the raw material needs for producing textile fibers, thread sacks, paper, and ropes. In the U.S. alone, the overall value of hemp production totaled $824 million in 2021; in the coming years, the production rate is only set to grow drastically. In 2022, the amount of hemp grown in the U.S. only for extracting fibers is estimated to be $28.3 million dollars. From ancient times, hemp has been used as a major source for the extraction of fibers from their stems to a great extent, where the ships in the Columbian era would not have been able to operate without the strong and durable ropes and masts made from hemp fibers.[16−19] When hemp fibers are produced from the hemp hurd, about 80% is left as residue which needs proper disposal.[20] The hemp stem waste, being rich in lignin and cellulose, is an ideal precursor for synthesizing biochar and brings in more economic benefits along with enhanced sustainability for hemp crops.[21−23]

Over the past decade, biochar-based carbon materials have replaced conventional polymer composite fillers, such as carbon nanotubes and graphene-based materials produced using synthetic methods, due to their economic viability, environmental friendliness, and relatively easy synthesis. The main objectives of biochar carbon reinforcement are to improve the mechanical, thermal, and electrical properties of the polymer matrix. Even when compared with polymer composites reinforced with natural fillers, biochar-reinforced composites were found to have superior properties. The surface properties of biochar play a prominent role in polymer composites when used as fillers. Altering the biochar surface can considerably enhance their interaction and adhesion to the polymer matrix, which helps in the overall property enhancement of the composite. Even though the properties of biochar can be greatly modified to an extent by altering the pyrolysis process parameters, for effective modifications other chemical treatments are often preferred.[24] Surface functionalization is also considered efficient in preventing agglomeration phenomenon which is common for micro- or nanosized materials. Various surface functionalization techniques are being used, and most of them involve wet chemical approaches, which are often not eco-friendly and are effortful. In our recent study, low-temperature plasma treatment (LTP) has also been found effective in surface modification by introducing various functional groups on the surface.[25,26] LTP is composed of highly energetic excited electronic species, such as ions, electrons, and radicals. The collision of these particles on the surface is found to not only alter the physical properties but also to introduce functional groups, thus enhancing the overall reactivity of the material.[25]

Since the inert surface nature of carbon-based materials has been a major drawback when used as fillers, researchers have started utilizing LTP to address this problem. Fluorine functionalization of carbon has also been found to be an effective strategy when used as fillers to enhance the overall performance of composite materials. Mohammed et al. demonstrated the effect of fluorination by means of LTP on biochar synthesized from starch. The LTP treatment was found promising in attaching fluorine functionalities and improved the overall properties of composites when used as fillers.[26] Similarly, Shofner et al. and McIntosh et al. also found that the fluorination of carbon nanotube walls was very helpful in improving their interfacial interaction with the polymer matrices in which they are reinforced.[27,28]

The objective of the present study is to improve the sustainability of waste HDPE plastics and hemp stem waste (HSW) by reinforcing HSW-derived carbon in the waste HDPE matrix for the synthesis of films for packaging applications. Carbon was synthesized from hemp stem waste by using a pyrolysis process. The effect of low-temperature plasma treatment in the presence of sulfur hexafluoride gas on carbon fillers was also studied. Incorporating plasma treatment enhanced the overall improvement of crystallinity and mechanical strength of the composite films.

EXPERIMENTAL SECTION

Materials. HDPE Walmart waste distilled water cans were chosen for the experiment. The waste cans were collected, cleaned, and cut into small films. The hemp stem waste, used as a precursor for synthesizing carbon, was procured from Tuskegee University's agricultural department.

Methods. *Synthesis and Functionalization of Carbon.* The biochar carbon was synthesized from hemp stem wastes by means of the pyrolysis method. HSW was subjected to elevated temperatures from room temperature to 850 °C at a heating rate of 5 °C/min using an MTI autogenic pressure high-temperature reactor under a nitrogen environment. During the synthesis, HSW was kept at 850 °C for 2.5 h for effective graphitization. Plasma Etch PE 100 equipment was used to functionalize the carbon synthesized from HSW. The equipment was custom designed and built with a rotating sample drum, which ensures uniform treatment for the samples. The carbon was subjected

https://doi.org/10.1021/acssusresmgt.3c00041
ACS Sustainable Resour. Manage. 2024, 1, 625−633

to low-temperature plasma treatment under a sulfur hexafluoride (SF_6) environment for 10 min for effective functionalization. The untreated and plasma-treated carbon was named "Neat HC" and "SF_6 10 HC", respectively.

X-ray diffraction (XRD) analysis. XRD analysis of the carbon samples was carried out using the Rigaku Smart lab Studio II system with Cu Kα radiation (α = 0.154 nm) at 45 kV, 40 mA, and 1800 kW. The diffraction data were collected within 2θ ranging from 10 to 75° at a scan speed of 1°/ min with a step size of 0.01°.

Raman Spectroscopy. The graphitization and defects associated with the carbon samples were studied by conducting Raman spectroscopy using Thermo Scientific DXR Raman spectroscopy equipped with a laser source of excitation wavelength of 785 nm. The spectrum was obtained within the wavelength range of 500−2500 cm^{-1} by 128 scans at a spectral resolution of 4 cm^{-1}.

X-ray Photoelectron Spectroscopy (XPS). The surface functionalities and elemental composition of the carbon samples were studied by using Phi Electronics, Inc. equipment with VersaProbe 5000, having a monochromatic Al X-ray source with 100 μm spot size at a power of 25 W.

Fourier Transform Infrared (FTIR) Spectroscopy. The FTIR spectrum of the carbon samples was obtained using a Shimadzu IRTracer-100 spectrophotometer in transmittance mode over wavelengths ranging from 500 to 4000 cm^{-1} at a resolution of 4 cm^{-1}.

Textural properties. The textural properties of carbon samples were studied using a Quantachrome Autosorb iQ station. The samples were vacuum degassed at 120 °C overnight to eliminate volatiles. The adsorption−desorption isotherms of the samples with nitrogen at 77 K were within the partial pressure range starting from 0.025 to 0.99. The adsorption isotherms were used to calculate the surface areas of the samples. The surface area of the samples was calculated from multipoint BET tests. The pore volume and size were determined by the nonlinear density functional theory (DFT) method.

Scanning Electron Microscopy (SEM) Analysis. The surface morphology and microstructure of the carbon samples were analyzed by using field emission-SEM (Jeol-7200F). The carbon samples were sonicated in ethanol for a few minutes to reduce their agglomeration behavior and were later spread onto carbon tape, which was attached to the aluminum stubs. The carbon tape, along with the samples on them, was subjected to sputtering with Pd/Au before the SEM analysis to inhibit charging, which can likely occur when the electron beam strikes the sample surface.

Composite Film Fabrication. The cut waste HDPE pieces with average dimensions of 10 mm in length and breadth were mixed well with plasma-treated and untreated carbon separately at different weight percentage loadings of 0.25, 0.5, 1, and 2 wt %, respectively, until the films were uniformly coated with the carbon. A few drops of poly(ethylene glycol) as a plasticizer also helped ensure the proper attachment of the carbon onto the surface of the cut HDPE pieces. The cut pieces coated with carbon were later subjected to melt extrusion for uniform dispersion and converted into films using Labtech microblown film extruder setup at a temperature of 145° C. The extruded films had an average thickness of 0.05 mm. The film samples were named as in Table 1.

HDPE/Carbon Composite Film Characterization. *Differential Scanning Calorimetry (DSC) Analysis.* DSC analysis was conducted on the composite films using TA Instruments Q2000 DSC for studying the thermal behavior of the films in non-isothermal mode at a heating rate of 10 °C/min from 30 to 250 °C and was cooled back to 30 °C using an external event at a cooling rate of 10 °C/min. The analysis was carried out in aluminum pans containing film samples against an empty reference pan. The analysis was conducted under a nitrogen atmosphere to maintain the inertness.

Thermogravimetric Analysis (TGA). TA Q500 TGA analyzer was used to study the thermal stability of films. The experiment was carried out in a nitrogen atmosphere by heating the samples from room temperature to 700 °C at a heating rate of 5 °C/min.

Tensile Tests. Mechanical properties of the films were studied by carrying out tensile tests using a Zwick Roell Z2.5 universal testing machine. The tests were conducted following the ASTM D882 standard, and a 2.5 kN load cell was used to test the films. The tensile tests were carried out with a crosshead speed of 20 mm/min, and 5 samples were tested from each sample set.

Table 1. Sample Labels and Details

Sample no.	Film sample label	Description
1	Neat HDPE	HDPE film without any carbon reinforcement
2	HDPE/0.25 wt % HC	HDPE film reinforced with 0.25 wt % untreated hemp carbon
3	HDPE/0.5 wt % HC	HDPE film reinforced with 0.5 wt % untreated hemp carbon
4	HDPE/1 wt % HC	HDPE film reinforced with 1 wt % untreated hemp carbon
5	HDPE/2 wt % HC	HDPE film reinforced with 2 wt % untreated hemp carbon
6	HDPE/0.25 wt % SF_6 10 HC	HDPE film reinforced with 0.25 wt. % plasma-treated hemp carbon
7	HDPE/0.5 wt % SF_6 10 HC	HDPE film reinforced with 0.5 wt % plasma-treated hemp carbon
8	HDPE/1 wt % SF_6 10 HC	HDPE film reinforced with 1 wt.% plasma-treated hemp carbon.
9	HDPE/2 wt % SF_6 10 HC	HDPE film reinforced with 2 wt % plasma-treated hemp carbon

Fracture Surface Analysis. The fracture surface of the films subjected to tensile tests was analyzed using Jeol-7200F FE SEM. The fractured films were attached to the SEM sample holder in a vertical manner, which ensures the best visibility of the fracture surface and were subjected to sputtering to avoid the charging phenomenon.

RESULTS AND DISCUSSIONS

XRD pattern in Figure 1a revealed the graphitic nature of the hemp-derived carbon. Both [002] and [101] peaks at angles 24.63° and 43.56° represent the graphitic planes in the carbon.[29] Graphite is an allotrope of carbon, with multiple layers of graphene stacked together in a hexagonal structure. It is a known fact that defects or changes in the interplanar distances in graphite can result in shifting in peaks.[30] By subjecting the hemp carbon is subjected to plasma in the presence of SF_6 gas, it is evident that there is a small and relatively sharp peak formed at an angle of 18.98°. This can be due to the defects and deposition of fluorine atoms between the layers of the graphitic planes on the surface edges of the carbon, thus causing an intercalation effect. The intercalation of graphite for its effective exfoliation has been a topic of interest among researchers for a long time. Since the interplanar van der Waal's attraction force is high for graphite, researchers applied external forces through various methods to separate these planes effectively.[31] The new peak formation in the case of plasma-treated hemp carbon shows that the low-temperature plasma treatment has been able to separate the planes to an extent and, under optimized treatment conditions, can be a promising addition to the existing graphite exfoliation methods.

The Raman spectrum represented in Figure 1b also evidently shows the graphitic nature of the samples. The D band and G band peaks indicating the presence of graphite can be found at wavelengths of ∼1315 and ∼1586 cm^{-1}, respectively. The G and D bands correspond to the bonding vibrations arising from the sp^2 hybridization and sp_3 hybridization, respectively. It can be noted that there is a significant presence of D and G bands in both untreated and plasma-treated carbon samples, which indicates that the carbon synthesized is not graphite in its pristine form, having sp^2 hybridization only. However, compared to the untreated

https://doi.org/10.1021/acssusresmgt.3c00041
ACS Sustainable Resour. Manage. 2024, 1, 625−633

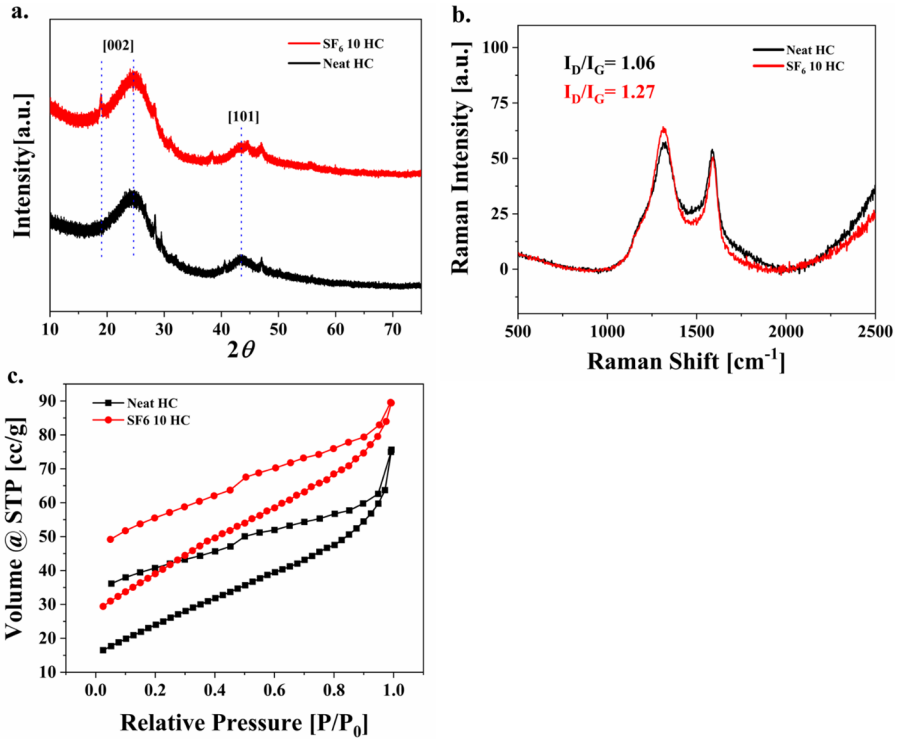

Figure 1. (a) XRD spectrum of the neat HC and SF_6 10 HC and (b) Raman spectrum of the neat HC and SF_6 10 HC and (c) nitrogen adsorption−desorption isotherm.

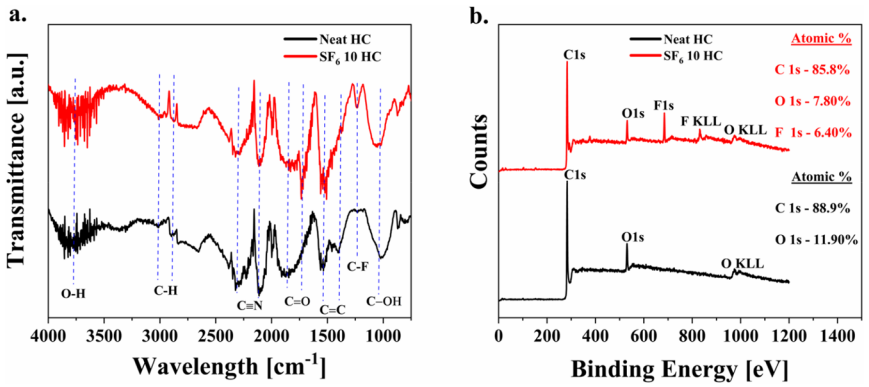

Figure 2. (a) FTIR spectrum of the neat HC and SF_6 10 HC and (b) XPS spectrum of the neat HC and SF_6 10 HC.

carbon, the intensity of the D band was observed to increase with the plasma treatment, which can be attributed to the additional radical sp^3 carbon sites created on the carbon surface during their interaction with highly energetic electronic species in the plasma and the formation of C−F bonds. The I_D/I_G ratio, which is significant for graphitic carbon materials for estimating the defect density, also increased from 1.06 to 1.27 due to plasma treatment.[32] The BET results are listed in Figure 1c. There has been a significant increase in the surface area of carbon with plasma treatment. Both samples had a type IV isotherm associated with the capillary condensation phenomenon in multilayered mesoporous materials. The surface area of the hemp-derived carbon increased from 81.08 to 123.40 m^2/g because of the plasma treatment. However, changes in the pore size (1.688 to 1.542 nm) and pore volume (0.094 to 0.121 cc/g) were not that significant. Based on the Raman spectra and BET results, it could be hypothesized that the LTP treatment is not introducing defects of porous nature on the carbon. However, there should be other alterations on the carbon surface resulting from the LTP treatment which translated into improving surface area.[33,34]

From the FTIR spectrum of the carbon shown in Figure 2a, in the spectrum of SF_6-treated carbon, there is a peak at a wavelength of ∼1230 cm^{-1}, which represents the C−F vibrations. This further confirms the fact that the interaction of fluorine ions in the plasma with the sp^3 hybridized carbon radicals on the surface created covalent C−F bonds with them. The shift of the peak representing the C−F bond from lower wavelengths to upper wavelengths is generally attributed to their increased covalent behavior. Since the peak representing C−F vibrations here is in the higher wavelength range, at ∼1230 cm^{-1}, it has a covalent nature. Hence, with FTIR studies, it is evident that carbon−fluorine characteristics are introduced into carbon with the plasma treatment. Apart from the formation of the C−F peak, other major relevant

https://doi.org/10.1021/acssusresmgt.3c00041
ACS Sustainable Resour. Manage. 2024, 1, 625−633

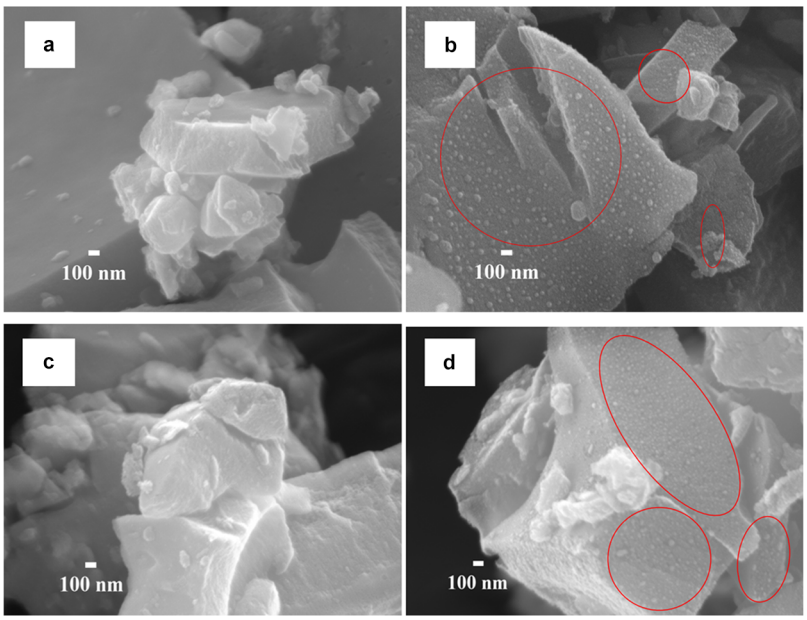

Figure 3. SEM micrographs of (a, c) neat HC and (b, d) SF_6 10 HC.

differences in the samples were not observed with the plasma treatment.[35,36]

The XPS spectrum in Figure 2b suggested a strong presence of fluorine along with a reduction of oxygen in the plasma-treated carbon sample. The introduction of fluorine to carbon can potentially influence the hydrophilic characteristics of the carbon surface, which need further investigation. The fluorine atomic percentage in carbon was found to increase from 0 to 6% because of plasma treatment. The reduction in atomic percentages of carbon and oxygen can also be attributed to the etching that happened during the plasma treatment.[37]

The morphological changes of the carbon due to the plasma treatment were analyzed using SEM and are shown in Figure 3. The synthesized carbon had a layer-like graphitic structure, which can be seen in Figure 3. The size of the particles was irregular, and the average size of the particles was less than 100 μm. Panels b and d of Figure 3 show the dot-like structures (which can be seen mostly in the red markings) formed on the carbon due to the plasma treatment, which could have formed as a result of the defects created while etching during the interaction with the excited fluorine ions. Since the other characterizations strongly suggest the formation of fluorine functionalities on the surface, these dot-like structures could also be the sites where they have been introduced. The morphological images correlate well with the BET results of the carbon samples and prove our hypothesis that the enhancement of the surface area of carbon subjected to LTP treatment is mainly due to dot-like protruding structures formed on the carbon. Since there is the presence of these nanoscale protrusions on the surface of the plasma-treated carbon, the surface area available for interaction when used as fillers in a matrix would be relatively more than the untreated carbon and should enhance other properties, when used as fillers. Overall, the plasma-treated carbon had a rougher morphology compared to that of the untreated carbon. Briefly, based on the studies conducted on the plasma treated and untreated carbon, the highly energetic fluorine ions and electrons present in the plasma are striking the carbon surface which etch out the carbon atoms and will create sp^3 carbon sites. These newly created sp^3 hybridized carbon sites present on the surface will bond with the fluorine ions present in the plasma sheath and create C−F covalent bonds. These chemical changes later lead to further alterations in the physical properties of carbon, such as morphology and surface area.

Figure 4 and Table 2 represent the thermogravimetric analysis results of the HDPE films reinforced with carbon conducted to study thermal stability. The decomposition onset temperature was found to increase relatively with the carbon loading increments in the matrix, and the thermal stability of the polymer was enhanced with the reinforcement.

The thermal behavior and crystallinity were studied by using DSC, and the curves are illustrated in Table 3, Table 4, and Figure 5. The melting point of the films was found to have a decreasing trend with the addition of untreated carbon. However, there was an opposite trend in the case of plasma-treated carbon-reinforced films, with a significant increase in their melting point. The melting enthalpy was also on the higher side for the plasma-treated carbon-reinforced films when compared to the untreated carbon-reinforced films. When fillers are reinforced into a polymer matrix, it is natural that the cross-linking will be enhanced and the mobility of polymer chains will be restricted. Here, in addition to adding fillers, fillers were further modified before reinforcement by introducing fluorine functionalities and altering the surface morphology. Moreover, with fluorine being an element of higher electronegativity order, during the extrusion, it could pull more electronic species toward them and act as active cross-linking agents in the polymer matrix, promoting nucleation and crystallite growth. The crystallization temperature was not changed significantly with the incorporation of carbon, but the crystallization enthalpy was higher for the composite films.

The crystallinity percentage was calculated based on the melting enthalpy associated with each sample using the equation below.

$$\text{crystallinity } \% = \frac{\Delta H_m}{(1-\varphi)\Delta H^\circ_m}$$

https://doi.org/10.1021/acssusresmgt.3c00041
ACS Sustainable Resour. Manage. 2024, 1, 625−633

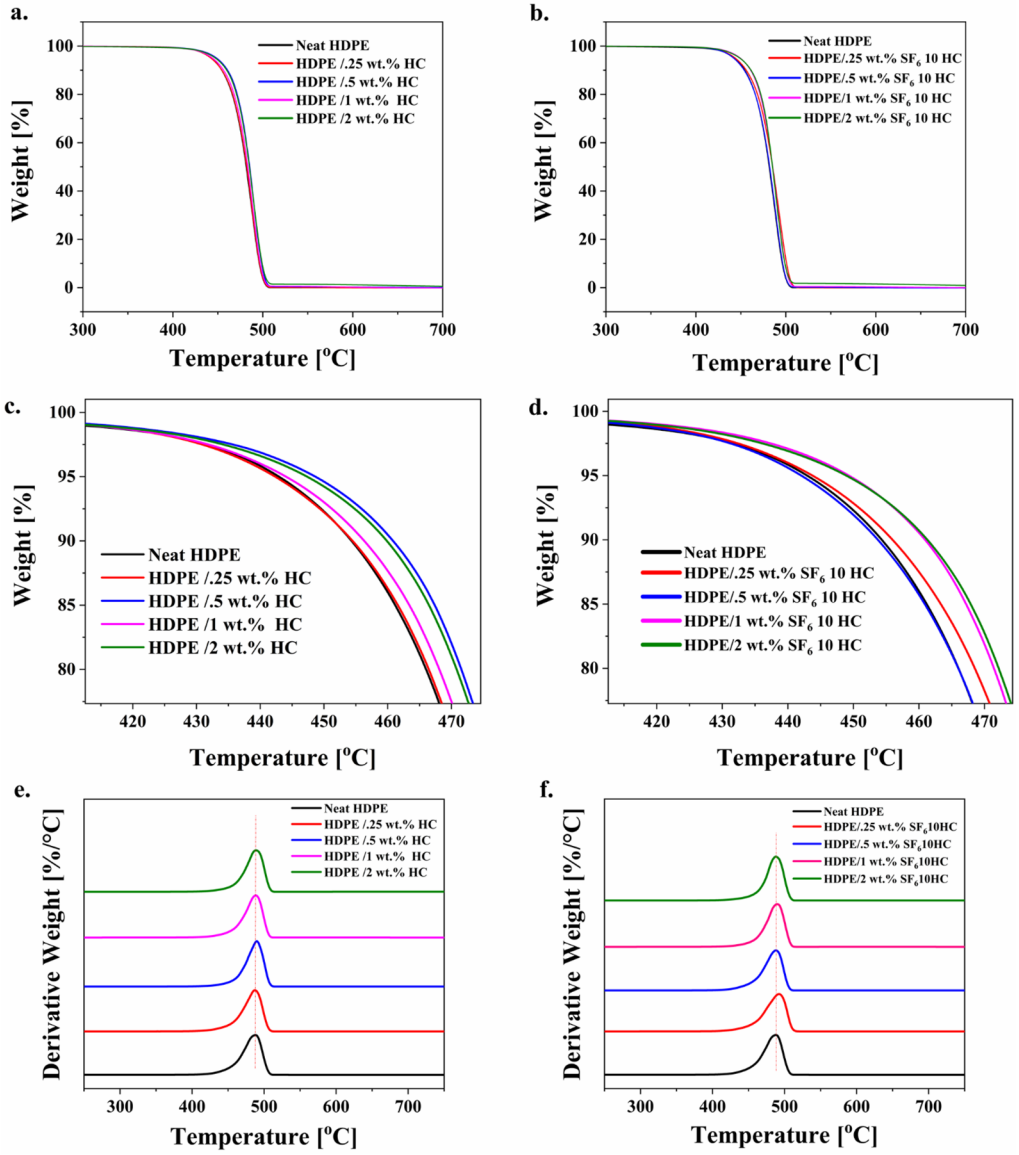

Figure 4. TGA curves of the HDPE/carbon composite films: (a, b) weight versus temperature curves of the composite films; (c, d) enlarged versions of panels a and b representing the onset of decomposition behavior of the films; and (e, f) weight derivative versus temperature curves.

Table 2. TGA Analysis Results of the Film Samples

Sample no.	Film samples	Decomposition onset temp (°C)	Max decomposition temp (°C)
1	Neat HDPE	464.52	487.90
2	HDPE/0.25 wt % HC	466.01	490.86
3	HDPE/0.5 wt % HC	470.88	488.52
4	HDPE/1 wt.% HC	467.34	488.53
5	HDPE/2 wt % HC	468.68	488.63
6	HDPE/0.25 wt % SF_6 10 HC	465.60	489.54
7	HDPE/0.5 wt % SF_6 10 HC	465.18	487.90
8	HDPE/1 wt.% SF_6 10 HC	469.38	489.39
9	HDPE/2 wt % SF_6 10 HC	469.83	487.72

where ΔH_m and ΔH°_m are the melting enthalpies of the composite and 100% crystalline HDPE, respectively, and φ is the weight fraction of the reinforced carbon in the composites. The crystallinity % represented in Table 4 was enhanced significantly upon the addition of carbon. Even though the addition of untreated carbon to the HDPE system enhanced the crystallinity% considerably, the films with the plasma-treated carbon had a further increase in crystallinity % because of the increased cross-linking and the interface interaction between the fillers and the matrix. These improvements in crystallinity % and thermal stability strongly suggest the absence of agglomeration and uniform dispersion of the carbon in the HDPE matrix. High melting enthalpy of the composite

https://doi.org/10.1021/acssusresmgt.3c00041
ACS Sustainable Resour. Manage. 2024, 1, 625−633

Table 3. Melting Point and Crystallization Temperature of the HDPE/Carbon Composite Films

Sample no.	Film sample	Melting point (°C)	Crystallization temp (°C)
1	Neat HDPE	135.03	116.45
2	HDPE/0.25 wt % HC	131.55	116.44
3	HDPE/0.5 wt % HC	133.34	116.69
4	HDPE/1 wt % HC	133.38	116.85
5	HDPE/2 wt % HC	133.90	114.38
6	HDPE/0.25 wt % SF_6 10 HC	134.23	117.45
7	HDPE/0.5 wt % SF_6 10 HC	138.84	116.54
8	HDPE/1 wt % SF_6 10 HC	138.35	115.99
9	HDPE/2 wt % SF_6 10 HC	133.95	115.45

Table 4. Melting Enthalpy and Crystallinity % of the HDPE/Carbon Composite Films

Sample no.	Film sample	Melting enthalpy (J/g)	Crystallinity %
1	Neat HDPE	133.5	45.56
2	HDPE/0.25 wt % HC	166.1	56.83
3	HDPE/0.5 wt % HC	181.3	62.18
4	HDPE/1 wt % HC	174.7	60.22
5	HDPE/2 wt % HC	176.9	61.60
6	HDPE/0.25 wt % SF_6 10 HC	158.3	54.16
7	HDPE/0.5 wt % SF_6 10 HC	184.9	63.42
8	HDPE/1 wt % SF_6 10 HC	186.9	64.43
9	HDPE/2 wt % SF_6 10 HC	187.1	65.41

films also signifies high restriction in polymer chain motion due to the addition of carbon fillers.[38]

The tensile test results of the films shown are illustrated in Figure 6 and Table 5. As a result of surface functionalization and improvement in the surface area available for the interfacial interaction, the films reinforced with plasma-treated carbon have relatively high mechanical strength and modulus. However, it can be noted that the strain % at fracture has considerably dropped, which could be attributed to the regular phenomenon found in polymer systems when their polymer chain stacking and cross-linking behavior is enhanced.[39] Also, it can be noted that the improvement of mechanical properties aligns well with the improvement observed in the thermal properties of the films, especially crystallinity.

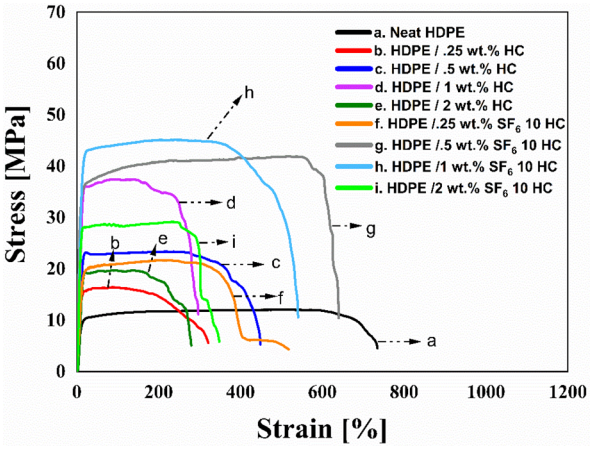

Figure 6. Tensile test curves of the HDPE/carbon composite films: (a) neat HDPE, (b) HDPE/0.25 wt % HC, (c) HDPE/0.5 wt % HC, (d) HDPE/1 wt % HC, (e) HDPE/2 wt % HC, (f) HDPE/0.25 wt % SF_6 10 HC, (g) HDPE/0.5 wt % SF_6 10 HC, (h) HDPE/1 wt % SF_6 10 HC, and (i) HDPE/2 wt % SF_6 10 HC.

In the HDPE films reinforced with untreated carbon, the compatibility between the carbon and the HDPE matrix would be very low, implying weak connection between carbon and HDPE. When there is weak connection between the filler and the matrix, application of external load in the same direction of crack propagation would lead to earlier interface delamination, so to resist this phenomenon, it is necessary to have strong interfacial interaction between the fillers and the polymer matrix. The improvement in mechanical properties here in the case of HDPE composites reinforced with plasma-treated carbon when compared to the latter reinforced with untreated carbon portrays the importance of strong interfacial interaction very well.[40] Overall, the improvement in the mechanical properties strongly supports the fact that surface modification of the carbon by means of plasma significantly helped to enhance the interface adhesion. The fracture surface of the films was analyzed using SEM, which is represented in Figure 7. Compared with the neat HDPE film fracture surface in Figure 7A, the composite films (Figure 7b,c) had more fibrous pullouts and nucleation sites. It is evident that the fillers played a major role in uniformly distributing the load and restricting the films from easy fracture. Also, the fracture surface of the films reinforced with plasma-treated carbon (Figure 7c) was

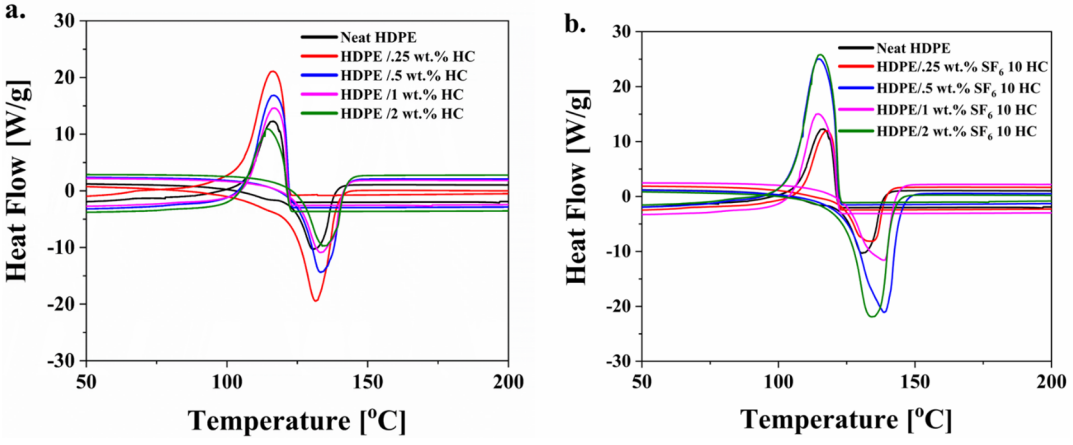

Figure 5. DSC curves of the HDPE/carbon composite films: (a) untreated and (b) plasma treated.

https://doi.org/10.1021/acssusresmgt.3c00041
ACS Sustainable Resour. Manage. 2024, 1, 625−633

Table 5. Tensile Results of the HDPE/Carbon Composite Films

Sample no.	Film samples	Max strength (MPa)	Elastic modulus (MPa)	Strain % at fracture
1	Neat HDPE	12.06 ± 0. 913	1.04 ± 0.085	734.62 ± 12.0
2	HDPE/0.25 wt % HC	16.45 ± 0.842	1.85 ± 0.069	320.61 ± 5.80
3	HDPE/0.5 wt % HC	32.90 ± 1.124	2.54 ± 0.127	448.96 ± 7.50
4	HDPE/1 wt % HC	37.43 ± 1.532	2.98 ± 0.074	296.99 ± 10.60
5	HDPE/2 wt % HC	19.74 ± 0.951	3.45 ± 0.091	279.54 ± 5.53
6	HDPE/0.25 wt % SF_6 10 HC	21.70 ± 0.760	1.68 ± 0.009	518.08 ± 8.67
7	HDPE/0.5 wt % SF_6 10 HC	41.91 ± 1.453	3.01 ± 0.065	639.86 ± 7.13
8	HDPE/1 wt % SF_6 10 HC	45.16 ± 0.967	3.62 ± 0.117	540.67 ± 10.10
9	HDPE/2 wt % SF_6 10 HC	29.16 ± 0.089	3.45 ± 0.093	347.43 ± 6.68

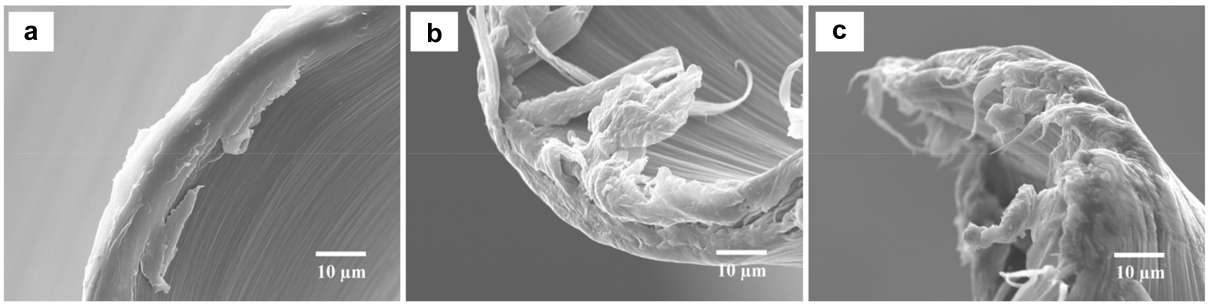

Figure 7. SEM micrographs of the fractured surfaces of (a) neat HDPE film, (b) 1 wt % HC reinforced HDPE film, and (c) 1 wt % SF6 10 HC reinforced HDPE film.

found to have a tougher fracture than the rest, accounting for the relatively high crystallinity and brittle behavior.

CONCLUSION

Waste HDPE distilled water cans were successfully upcycled into composite films for packaging applications with the reinforcement of carbon synthesized from hemp stem waste by employing the pyrolysis technique. In addition, biochar carbon, generally considered inert, was successfully surface functionalized using low-temperature plasma treatment, which resulted in the introduction of fluorine functionalities and improvement in the surface area available for the matrix−filler interfacial interaction. The major changes associated with the plasma-treated carbon when compared to the untreated carbon are the improvement in surface area, the presence of C−F bonds, and the morphological alterations, such as the development of dot-like structures on the carbon surface. Incorporating plasma-treated carbon as fillers proved to be a potential technique for enhancing the overall properties of the composite as both thermal and mechanical properties improved significantly. The crystallinity % of the polymer matrix was considerably enhanced with the reinforcement of plasma-treated carbon, which further translated to improvement in the mechanical properties of the composite as well. Proportional to the increment in crystallinity, a drop in the strain was also observed, making the films more brittle. The composite films loaded with plasma-treated 1 wt % carbon had superior mechanical and thermal properties compared to other samples, which could be attributed to the improved matrix−filler interfacial properties. In conclusion, this work successfully portrayed a potential method for upcycling HDPE waste by reinforcing functionalized biochar carbon by incorporating low-temperature plasma technology.

AUTHOR INFORMATION

Corresponding Author

Vijaya Rangari − *Department of Materials Science & Engineering, Chappie James Hall, Tuskegee University, Tuskegee, Alabama 36088, United States;* orcid.org/0000-0002-3962-1686; Email: vrangari@tuskegee.edu

Authors

Gautam Chandrasekhar − *Department of Materials Science & Engineering, Chappie James Hall, Tuskegee University, Tuskegee, Alabama 36088, United States*

Kearston Edwards − *Department of Chemical Engineering, Tuskegee University, Tuskegee, Alabama 36088, United States*

Desmond Mortley − *Department of Agricultural & Environmental Sciences, Tuskegee University, Tuskegee, Alabama 36088, United States*

Complete contact information is available at: https://pubs.acs.org/10.1021/acssusresmgt.3c00041

Notes

The authors declare no competing financial interest.

ACKNOWLEDGMENTS

The authors acknowledge the constant financial support of NSF AL-EPSCoR #2148653, NSF-CREST #1735971, and the Al-EPSCoR- GRSP Fellowship. The authors also acknowledge Dr. Sohini Bhattacharyya, Dr. P. M Ajayan, and Ajayan Research Group from the Department of Materials Science and Nanoengineering at Rice University, Houston, TX, USA, for helping us with textural characterization techniques.

REFERENCES

(1) Hopewell, J.; Dvorak, R.; Kosior, E. Plastics recycling: Challenges and opportunities. *Philos Trans. R. Soc., B* **2009**, *364*, 2115−2126.

(2) MacArthur, D. E. Beyond plastic waste. *Science* **2017**, *358*, 843.
(3) Vollmer, I.; et al. Beyond Mechanical Recycling: Giving New Life to Plastic Waste. *Angew. Chem., Int. Ed.* **2020**, *59*, 15402−15423.
(4) Garcia, J. M.; Robertson, M. L. The future of plastics recycling. *Science* **2017**, *358*, 870−872.
(5) Ignatyev, I. A.; Thielemans, W.; Vander Beke, B. Recycling of polymers: A review. *ChemSusChem* **2014**, *7*, 1579−1593.
(6) Chopra, S., Pande, K., Kumar, V. S., Sharma, J. A., Eds. *Novel Applications of Carbon Based Nano-Materials* CRC Press, 2022. DOI: 10.1201/9781003183549.
(7) Kumar, S.; Panda, A. K.; Singh, R. K. A review on tertiary recycling of high-density polyethylene to fuel. *Resour., Conserv. Recycl.* **2011**, *55*, 893−910.
(8) Kumar, S.; Singh, R. K. Thermolysis of High-Density Polyethylene to Petroleum Products. *J. Pet. Eng.* **2013**, *2013*, 1−7.
(9) Ravindra, K.; Singh, T.; Mor, S. Emissions of air pollutants from primary crop residue burning in India and their mitigation strategies for cleaner emissions. *J. Clean. Prod.* **2019**, *208*, 261−273.
(10) Venkataraman, C. Emissions from open biomass burning in India: Integrating the inventory approach with high-resolution Moderate Resolution Imaging Spectroradiometer (MODIS) active-fire and land cover data. *Global Biogeochem. Cycles* **2006**, *20*, GB2013.
(11) Azeta, O.; Ayeni, A. O.; Agboola, O.; Elehinafe, F. B. A review on the sustainable energy generation from the pyrolysis of coconut biomass. *Sci. Afr.* **2021**, *13*, e00909.
(12) Koul, B.; Yakoob, M.; Shah, M. P. Agricultural waste management strategies for environmental sustainability. *Environ. Res.* **2022**, *206*, 112285.
(13) Chowdhury, Z. Z. Preparation of carbonaceous adsorbents from lignocellulosic biomass and their use in removal of contaminants from aqueous solution. *BioResources* **2013**, *8*, 6523−6555.
(14) Bartoli, M.; Arrigo, R.; Malucelli, G.; Tagliaferro, A.; Duraccio, D. Recent Advances in Biochar Polymer Composites. *Polymers* **2022**, *14*, 2506.
(15) Mi, J.; Wang, X. R.; Fan, R. J.; Qu, W. H.; Li, W. C. Coconut-shell-based porous carbons with a tunable micro/mesopore ratio for high-performance supercapacitors. *Energy Fuels* **2012**, *26*, 5321−5329.
(16) Cherney, J. H.; Small, E. Industrial hemp in North America: Production, politics and potential. *Agronomy* **2016**, *6*, 58.
(17) *U.S. Billion-Ton Update: Crop Residues and Agricultural Wastes*; United States Department of Energy, 2011.https://www1.eere.energy.gov/bioenergy/pdfs/btu_crop_residues.pdf (Accessed July 26th 2023).
(18) *National Hemp Report*; United States Department of Agriculture, 2022https://www.nass.usda.gov/Newsroom/Executive_Briefings/2023/04-19-2023.pdf (Accessed July 26th 2023).
(19) *Commodities at a Glance: Special Issue on Industrial Hemp*; United Nations, 2022. https://unctad.org/system/files/official-document/ditccom2022d1_en.pdf (Accessed July 26th 2023).
(20) Liu, S.; et al. Activated carbon derived from bio-waste hemp hurd and retted hemp hurd for CO_2 adsorption. *Compos. Commun.* **2017**, *5*, 27−30.
(21) Yang, M.; et al. MnO_2 Nanowire/Biomass-Derived Carbon from Hemp Stem for High-Performance Supercapacitors. *Langmuir* **2017**, *33*, 5140−5147.
(22) Zhang, J.; Gao, J.; Chen, Y.; Hao, X.; Jin, X. Characterization, preparation, and reaction mechanism of hemp stem based activated carbon. *Results Phys.* **2017**, *7*, 1628−1633.
(23) Sun, W.; Lipka, S. M.; Swartz, C.; Williams, D.; Yang, F. Hemp-derived activated carbons for supercapacitors. *Carbon* **2016**, *103*, 181−192.
(24) Tengku Yasim-Anuar, T. A.; et al. Emerging application of biochar as a renewable and superior filler in polymer composites. *RSC Adv.* **2022**, *12*, 13938−13949.
(25) Mohammed, Z.; Jeelani, S.; Rangari, V. Low temperature plasma treatment of rice husk derived hybrid silica/carbon biochar using different gas sources. *Mater. Lett.* **2021**, *292*, 129678.
(26) Mohammed, Z.; Jeelani, S.; Rangari, V. K. Effect of Low-Temperature Plasma Treatment on Starch-Based Biochar and Its Reinforcement for Three-Dimensional Printed Polypropylene Biocomposites. *ACS Omega* **2022**, *7*, 39636−39647.
(27) Shofner, M. L.; Khabashesku, V. N.; Barrera, E. V. Processing and mechanical properties of fluorinated single-wall carbon nanotube-polyethylene composites. *Chem. Mater.* **2006**, *18*, 906−913.
(28) McIntosh, D.; Khabashesku, V. N.; Barrera, E. V. Nanocomposite fiber systems processed from fluorinated single-walled carbon nanotubes and a polypropylene matrix. *Chem. Mater.* **2006**, *18*, 4561−4569.
(29) Idrees, M.; Jeelani, S.; Rangari, V. Three-Dimensional-Printed Sustainable Biochar-Recycled PET Composites. *ACS Sustainable Chem. Eng.* **2018**, *6*, 13940−13948.
(30) Phillips, R.; Jolley, K.; Zhou, Y.; Smith, R. Influence of temperature and point defects on the X-ray diffraction pattern of graphite. *Carbon Trends* **2021**, *5*, 100124.
(31) Cai, M.; Thorpe, D.; Adamson, D. H.; Schniepp, H. C. Methods of graphite exfoliation. *J. Mater. Chem.* **2012**, *22*, 24992−25002.
(32) Pimenta, M. A.; et al. Studying disorder in graphite-based systems by Raman spectroscopy. *Phys. Chem. Chem. Phys.* **2007**, *9*, 1276−1291.
(33) Bardestani, R.; Patience, G. S.; Kaliaguine, S. Experimental methods in chemical engineering: specific surface area and pore size distribution measurements—BET, BJH, and DFT. *Can. J. Chem. Eng.* **2019**, *97*, 2781−2791.
(34) Zhang, J.; et al. Characteristics of biochar produced from yak manure at different pyrolysis temperatures and its effects on the yield and growth of highland barley. *Chem. Speciation Bioavailability* **2018**, *30*, 57−67.
(35) Wang, X.; et al. Characterization of Conformation and Locations of C-F Bonds in Graphene Derivative by Polarized ATR-FTIR. *Anal Chem.* **2016**, *88*, 3926−3934.
(36) Guérin, K.; et al. Synthesis and Characterization of Highly Fluorinated Graphite Containing sp2 and sp3 Carbon. *Chem. Mater.* **2004**, *16*, 1786−1792.
(37) Panomsuwan, G.; Saito, N.; Ishizaki, T. Simple one-step synthesis of fluorine-doped carbon nanoparticles as potential alternative metal-free electrocatalysts for oxygen reduction reaction. *J. Mater. Chem. A* **2015**, *3*, 9972−9981A.
(38) Poulose, A. M.; et al. Date palm biochar-polymer composites: An investigation of electrical, mechanical, thermal and rheological characteristics. *Sci. Total Environ.* **2018**, *619*−*620*, 311−318.
(39) Adeniyi, A. G. Prospects and problems in the development of biochar-filled plastic composites: a review. *Funct. Compos. Struct.* **2023**, *5*, 012002.
(40) Shirvanimoghaddam, K.; et al. Strategies to resolve intrinsic conflicts between strength and toughness in polyethylene composites. *Adv. Ind. Eng. Polym. Res.* **2023**, DOI: 10.1016/j.aiepr.2023.03.004.